



## Research article

# Bioactive components in *prunella vulgaris* for treating Hashimoto's disease via regulation of innate immune response in human thyrocytes

Yongzhao Chen<sup>a</sup>, Bo Jiang<sup>b</sup>, Cheng Qu<sup>b</sup>, Chaoyu Jiang<sup>b</sup>, Chen Zhang<sup>b</sup>, Yanxue Wang<sup>b</sup>, Fei Chen<sup>c</sup>, Xitai Sun<sup>d</sup>, Lei Su<sup>b,\*\*</sup>, Yuqian Luo<sup>e,\*</sup>

<sup>a</sup> Department of General Surgery, Nanjing Drum Tower Hospital, The Affiliated Hospital of Nanjing University of Chinese Medicine, Zhongshan Road 321, Nanjing, 210008, China

<sup>b</sup> Department of General Surgery, Nanjing Drum Tower Hospital, The Affiliated Hospital of Nanjing University Medical School, Zhongshan Road 321, Nanjing, 210008, China

<sup>c</sup> General Surgery Center, Department of Thyroid Surgery, Zhujiang Hospital, Southern Medical University 253 Gongye Middle Avenue, Haizhu District, Guangzhou, 510280, China

<sup>d</sup> Division of Pancreas and Metabolism Surgery, Department of General Surgery, Nanjing Drum Tower Hospital, The Affiliated Hospital of Nanjing University of Chinese Medicine, Nanjing, China, Zhongshan Road 321, Nanjing, 210008, China

<sup>e</sup> Clinical Medicine Research Center, Nanjing Drum Tower Hospital, The Affiliated Hospital of Nanjing University Medical School, Nanjing, China, Zhongshan Road 321, Nanjing, 210008, China

## ARTICLE INFO

## Keywords:

Hashimoto's thyroiditis  
*Prunella vulgaris*  
 Thyroid autoimmunity  
 Inflammation  
 Thyrocytes

## ABSTRACT

**Background:** Hashimoto's thyroiditis (HT) is a thyroid autoimmune disease characterized by lymphocytic infiltration and thyroid destruction. *Prunella vulgaris* (PV) is a traditional Chinese herbal medicine with documented clinical efficacy in treating HT. We previously reported an immunoregulatory effect of PV in thyrocytes; however, the bioactive components of PV remained unclear. This study aimed to elucidate key components of PV for treating HT and their acting mechanisms.

**Methods:** Network pharmacology was used to predict key PV components for HT. The predicted components were tested to determine whether they could exert an immunoregulatory effect of PV in human thyrocytes. Limited proteolysis-mass spectrometry (Lip-MS) was used to explore interacting proteins with PV components in human thyrocytes. Microscale thermophoresis binding assay was used to evaluate the affinity of PV components with the target protein.

**Results:** Eleven PV components with 192 component targets and 3415 HT-related genes were gathered from public databases. With network pharmacology, a 'component-target-disease' network was established wherein four flavonoids including quercetin, luteolin, kaempferol, morin, and a phytosterol,  $\beta$ -sitosterol were predicted as key components in PV for HT. In stimulated primary human thyrocytes or Nthy-ori-31 cells, key components inhibited gene expressions of inflammatory cytokines including tumor necrosis factor  $\alpha$  (TNF- $\alpha$ ), interleukin-6 (IL-6), and interferon- $\beta$  (IFN- $\beta$ ), cellular apoptosis, and activation of nuclear factor  $\kappa$ B (NF- $\kappa$ B) and interferon regulatory factor 3 (IRF-3). Heat shock protein 90 alpha, class A, member 1 (HSP90AA1), was identified to interact with flavonoids in PV by Lip-MS. Morin had the highest

\* Corresponding author.

\*\* Corresponding author.

E-mail addresses: [suleinjglyy@sina.com](mailto:suleinjglyy@sina.com) (L. Su), [yuqianluo31@foxmail.com](mailto:yuqianluo31@foxmail.com) (Y. Luo).

<https://doi.org/10.1016/j.heliyon.2024.e36103>

Received 3 June 2024; Received in revised form 5 August 2024; Accepted 9 August 2024

Available online 13 August 2024

2405-8440/© 2024 The Author(s). Published by Elsevier Ltd. This is an open access article under the CC BY-NC-ND license (<http://creativecommons.org/licenses/by-nc-nd/4.0/>).

affinity with HSP90AA1 ( $K_D = 122.74 \mu\text{M}$ ), followed by kaempferol ( $K_D = 168.53 \mu\text{M}$ ), luteolin ( $K_D = 293.94 \mu\text{M}$ ), and quercetin ( $K_D = 356.86 \mu\text{M}$ ).

**Conclusion:** Quercetin, luteolin, kaempferol, morin, and  $\beta$ -sitosterol reproduced an anti-inflammatory and anti-apoptosis effect of *PV* in stimulated human thyrocytes, which potentially contributed to the treatment efficacy of *PV* in HT.

## 1. Introduction

HT is a common thyroid autoimmune disease characterized by lymphocytic infiltration and thyroid destruction, which can result in enlarged nodules [1]. HT is often associated with hypothyroidism. So far there is no therapy to cure, ameliorate, or reverse thyroid inflammation and destruction in HT, though lifelong medication of synthetic thyroid hormone, i.e., levothyroxine (L-T4) works well to manage hypothyroidism. Risk factors of HT include both genetic and environmental ones [1]. Thyrocytes seem to play a suspicious role rather than simply being ‘an innocent victim’ of the lymphocytic infiltration in the pathogenesis of HT. It was proposed that activation of an innate immune response in thyrocytes might be initiating events for HT [2]. Upon exposure and recognition of pathogen-associated molecular patterns (PAMP) or danger-associated molecular patterns (DAMP), thyrocytes exert an innate immune response reflected by the production of various inflammatory cytokines, such as TNF- $\alpha$ , IL-6, IL-1 $\beta$ , and IFN- $\beta$  [2]. These pro-inflammatory cytokines could recruit lymphocytes to the thyroid, increasing the chance of breaking self-tolerance, particularly when genetic or environmental risk factors are also present. Moreover, when inflammation occurs, the function of thyrocytes is hindered and the cells even undergo dramatic cell death, possibly leading to thyroid destruction and hypothyroidism [2].

The herbal plant *PV* belongs to the genus *Prunella*. It can be eaten raw in salads, supplemented in beverages, and used in medication [3]. The anti-inflammatory and immune-regulating effects of *PV* have been well appreciated during the long-term practice of traditional Chinese medicine. *PV* has been used to treat thyroid diseases including HT, subacute thyroiditis, thyroid cysts, and thyroid adenoma [4]. For patients with subacute thyroiditis, combination therapy with *PV* had reduced prednisolone consumption [5]. Han et al. systematically reviewed evidence from 13 randomized controlled trials with 1468 thyroid nodule cases including HT [6]. They found that combination therapy with *PV* had more benefits for treating thyroid nodules, as it further decreased the nodule diameters and reduced the adverse reactions [6].

We previously showed that *PV* exerted an innate immune-modulating activity in stimulated rat thyroid FRTL-5 cells [7]. Aqueous *PV* extracts reduced double-stranded DNA (dsDNA) or dsRNA-induced gene expressions of inflammatory cytokines in FRTL-5 cells [7]. *PV* suppressed transactivation of transcription factors, NF- $\kappa$ B and IRF-3, in dsDNA/dsRNA-stimulated FRTL-5 cells [7]. *PV* also protected FRTL-5 cells from dsDNA/dsRNA-induced cell death [7]. The previous findings shed light on the mechanisms underlying *PV*'s beneficial effects on HT. However, the bioactive components responsible for *PV*'s effects remained unclear. In the present study, we investigated the potential pharmacodynamic materials and acting mechanisms of *PV* for treating HT using network pharmacology to predict the bioactive components with their disease targets. The predicted *PV* components were then tested to determine whether they could reproduce the innate immune-modulating and anti-apoptosis activities of *PV* in stimulated human thyrocytes. Moreover, we explored the proteins that interact with key *PV* components in inflamed human thyrocytes by Lip-MS approach and microscale thermophoresis binding assays.

## 2. Materials and methods

### 2.1. Network pharmacology analysis

The components of *PV* were obtained from TCMSP (<http://tcmspw.com/>), a database containing approximately 500 Chinese herbs and 30000 ingredients registered in the Chinese Pharmacopoeia [8]. The name of *PV* and its aliases were used as keywords. Two parameters from the absorption, distribution, metabolism, and excretion screening method (ADME): drug-likeness (DL) $\geq 0.18$  and oral bioavailability (OB) $\geq 30\%$  were used as criteria for screening the bioactive components of *PV* in the database [9]. The potential protein targets for the *PV* components and their interactions then retrieved from TCMSP database. Gene information of the targets was confirmed in Uniprot Knowledgebase (<https://www.uniprot.org>). The disease targets for HT were collected from the GeneCards database (<https://www.genecards.org/>) with a selection criterion of RiskScore  $> 1$ , OMIM (<https://www.omim.org/>), DrugBank (<https://go.drugbank.com/>), and PharmGKB (<https://www.pharmgkb.org/>).

The intersection of the targets of *PV* components and the disease targets were then obtained as the core targets of *PV* to treat HT. The core targets were imported into the STRING database (<https://string-db.org>) to construct a protein-protein interaction (PPI) network. Kyoto Encyclopedia of Genes and Genomes (KEGG) enrichment with the core targets of *PV* was performed in R studio using the ClusterProfiler package, and adjusted p-value (FDR)  $< 0.05$  was considered statistically significant.

The network of ‘component-target-disease’ was visualized using Cytoscape software [10]. In the network, nodes represent the bioactive components or targets, while edges represent the interactions between the nodes. The centrality degree of a node represents the number of edges it has in the network. To further screen key components of *PV*, the centrality degree of each node in the component-target interaction network and the PPI network was calculated using CytoNCA, a plug-in of Cytoscape software for network centrality analysis. The centrality degree was used to evaluate the importance of a node: the larger the degree value the more important the node is in the network.

The 3D protein structure of HSP90AA1 (with a co-crystal ligand) was obtained from the RCSB Protein Data Bank (<http://www.rcsb.org/pdb>). The molecular structures of PV components (i.e. potential ligands) were downloaded from PubChem (<http://pubchem.ncbi.nlm.nih.gov/>). To perform molecular docking analysis, the protein was first cleaned by deleting alternate conformations, adjusting the terminal residues, and correcting the bond orders. The 'cleaned' protein was then prepared using the "Prepare Protein" module of the "Macromolecules" tool in BIOVIA Discovery Studio (DS) (Dassault Systems, Vélizy-Villacoublay, France). Briefly, the water molecules were removed from the protein while keeping the protein intact together with its co-crystal ligand. CHARMM-based smart minimizer method at a maximum of 200 steps and 0.1 kcal mol<sup>-1</sup> RMSD gradient was also used to minimize the energy of the protein and potential ligands. Docking analysis was then performed using CDocker of BIOVIA DS.

## 2.2. Isolation of primary human thyrocytes

Human thyroid tissues were obtained from 10 donors during thyroid surgery with written consent. Cells from each donor were used independently for the experiment. Isolation of thyrocytes from tissues was performed as previously reported [11]. Briefly, fresh thyroid tissues were immersed in ice-cold Hank's Balanced Salt Solution (HBSS) in a 10 cm dish. Adipose and connective tissues were removed, and the remaining tissue was cut into 1–2 mm pieces with an ophthalmic scissor. Tissues were digested with 0.1 mg/ml collagenase IV (Sigma, St. Louis, MO) on an orbital shaker at 37 °C for 30 min. Digested fractions were filtrated through a 100 µm nylon filter, and washed twice in HBSS to remove the collagenase. Cells were pelleted by centrifugation at 200×g for 5 min and re-suspended in Dulbecco's Modified Eagle Medium (DMEM) supplemented with 10 % FBS (ThermoFisher Scientific, Waltham, MA).

## 2.3. Cell culture and treatment

Primary human thyrocytes were grown in DMEM containing 10 % FBS. Human thyroid Nthy-ori-31 cells were grown in RPMI-1640 containing 10 % FBS and 5 mM L-glutamine. Cells were stimulated after they had reached 80 % confluency. To induce an innate immune response in thyrocytes, 1 µg (for each well in a 6-well plate) or 0.1 µg (for each well in a 96-well plate) of synthetic dsDNA, i.e. poly (dA:dT) (#ttrl-patn, InvivoGen, San Diego, CA) or synthetic dsRNA, i.e. poly (I:C) (#ttrl-pic, InvivoGen) was transfected into cells using jetPRIME transfection reagents (Polyplus, Illkirch, France) according to the manufactory's instructions. Bioactive molecules of PV were all purchased from Sigma-Aldrich, St. Louis, MO; quercetin (#PHR1488), luteolin (#I9283), kaempferol (#K0133), and morin (#M4008) were dissolved in dimethyl sulfoxide (DMSO) and used at a final concentration of 10 µM (low-dose) or 40 µM (high-dose). While β-sitosterol (#S1270) was dissolved in ethanol (EtOH) and used at a final concentration of 50 µM (low-dose) or 150 µM (high-dose). Cells were stimulated with dsDNA or dsRNA in the presence or absence of bioactive molecule treatment at 37 °C in a CO<sub>2</sub> incubator for 6 h (only for protein assays) or 24 h, followed by RNA extraction, protein extraction, or apoptosis assays as described at below. Cells without dsDNA/dsRNA stimulation were used as controls in cellular functional assays.

## 2.4. RNA extraction and real-time PCR analysis

Total RNA was extracted from cells using TRIzol (Invitrogen, Carlsbad, CA), and cDNA was synthesized using HiScript III RT SuperMix kit (Vazyme, Nanjing, China) according to the manufactory's instructions. Real-time PCR was performed using the QuantStudio 5 Real-Time PCR System (ThermoFisher Scientific) and the Fast SYBR Green Master Mix (ThermoFisher Scientific). The primers used in the study include: *GAPDH* forward, 5'-ACAGCAACAGGGTGGTGGAC-3'; *GAPDH* reverse, 5'-TTTGAGGGTGCAGC-GAACTT-3'; *TNFα* forward, 5'-GACAAGCCTGTAGCCCATGT -3'; *TNFα* reverse, 5'-GACAAGCCTGTAGCCCATGT -3'; *IFNβ1* forward, 5'-TGCTCTCTGTTGTGCTTCTCCAC -3'; *IFNβ1* reverse, 5'-CAATAGTCTCATTCCAGCCAGTGC -3'; *IL6* forward, 5'-CTCAATATTA-GAGTCTCAACCCCA-3'; *IL6* reverse, 5'-GAGAAGGCAACTGGACCGAA-3'. A total of 10 ng cDNA mixed with 10 µL 2 × Fast SYBR Green Master Mix (ThermoFisher Scientific) was amplified by incubating for 20 min at 95 °C, followed by 40 cycles of 3 s at 95 °C and 30 s at 60 °C. Real-time PCR analysis was carried out in triplicate and the relative mRNA expression levels were normalized against *GAPDH* levels.

## 2.5. Caspase 3/7-mediated apoptosis assays by live-cell imaging

Incucyte NuLight red (Sartorius, Göttingen, Germany) and Incucyte Caspase 3/7 green (Sartorius) were used to label live cells and cells undergoing Caspase 3/7-mediated apoptosis, respectively. The addition of the Incucyte Caspase-3/7 dyes to normal healthy cells did not affect the cell growth or morphology. When added to the culture medium, the inert, non-fluorescent substrate crosses the cell membrane where it can be cleaved by activated Caspase-3/7 to release the fluorescent DNA dye. Live-cell imaging was captured for over 24 h and analyzed using Incucyte SX1 Live-Cell Analysis System (Sartorius), according to the manufacturer's instructions.

## 2.6. Protein extraction and Western blot analysis

Cells were lysed in RIPA Lysis Buffer (Beyotime, Shanghai, China) supplemented with protease and phosphatase inhibitor cocktail (Beyotime), according to the manufacturer's instructions. Total protein quantification was performed using the bicinchoninic acid (BCA) assay (Vazyme), and 10 µg of protein was used for Western blotting. Briefly, the proteins were separated on 10 % Bis-Tris gels by electrophoresis and transferred to the nitrocellulose membrane. The membrane was washed with tris-buffered saline (TBS) containing 0.1 % Tween 20 (TBST) and blocked in TBST containing 5 % bovine serum album (BSA) for 1 h. Then the membrane was incubated

with each primary antibody separately at 4 °C overnight. The primary antibodies used in this study include rabbit anti-phosphorylation nuclear factor of kappa light polypeptide gene enhancer in B cell inhibitor  $\alpha$  (pIkB- $\alpha$ ) (#AP0707, ABclonal Technology Co., Ltd., Wuhan, China), phosphorylation interferon regulatory factor 3 (pIRF-3) (#AP0995, ABclonal Technology Co., Ltd.), mouse monoclonal anti-GAPDH (HRP conjugated) (Beyotime), and mouse monoclonal anti- $\beta$ -Tubulin (HRP conjugated) (Beyotime). After washing with TBST, membranes were incubated with horseradish peroxidase (HRP)-labeled goat anti-rabbit IgG (Abcam, Cambridge, UK) as a secondary antibody. Specific proteins were visualized using an ECL chemiluminescence kit (Vazyme), and the chemiluminescence was detected using Tanon 5200 Chemi-Image System (ABclonal Technology Co., Ltd).

### 2.7. Identification of proteins interacting with flavonoids by limited proteolysis-mass spectrometry (Lip-MS)

Chemical proteomics using Lip-MS approach was performed as previously reported [12]. Briefly, primary human thyrocytes isolated from normal thyroid tissues were stimulated with 1  $\mu$ g of poly (dA:dT) or 1  $\mu$ g poly (I:C) at 37 °C in a CO<sub>2</sub> incubator for 6 h. The stimulated cells were lysed by bead-beating in PBS at 4 °C. After centrifugation at 16,000 $\times$ g for 10 min at 4 °C, the supernatant was collected and aliquoted in 6 equivalent volumes. To identify the proteins that interacted with flavonoids, 0.33 nmol/ $\mu$ g (total protein) of luteolin, morin, quercetin, or triplicates of the vehicle DMSO was added to each protein aliquot and incubated at 25 °C for 10 min. Limited proteolysis was conducted by digestion with protein kinase K (Sangon, Biotech, China) at a 1:100 enzyme/substrate ratio, followed by digestion with trypsin at a 1:50 enzyme/substrate ratio. The digested fragments were subjected to mass spectrometry analysis. Peptide fragments were analyzed by Nano Acuity Ultra-High Pressure liquid chromatography coupled with Thermo Q Exactive mass spectrometer (ThermoFisher Scientific). Proteins and peptides were identified using a target-decoy approach with a reversed database and queried against the Human UniProt FASTA database. The quantification of peptides and proteins with “label-free quantification” (LFQ) was performed by MaxQuant. Significant changes in the abundance of half-tryptic peptides (fold change (FC) > 2 or < 0.5,  $p < 0.05$ ) were read out between the DMSO-incubated samples and the flavonoid-incubated samples.

### 2.8. Microscale thermophoresis (MST) binding assay

Human HSP90AA1 protein (MedChemExpress, Monmouth Junction, NJ) was labeled with fluorescent His-tag using The Monolith His-tag Labeling Kit RED-tris-NTA (NanoTemper Technologies, Munich, Germany). Serial dilution of each ligand (quercetin, luteolin, kaempferol, morin, and,  $\beta$ -sitosterol) or DMSO/ethanol (as the vehicle) was prepared, ranged from 30 nM to 1 mM, and then incubated with 50 nM His-tag labeled HSP90AA1 protein for 10 min in the dark at room temperature in PBS buffer. The mixtures were loaded into the Nano Temper glass capillaries and detected by the microthermophoresis by MST (NanoTemper Technologies) according to the manufacturer's instructions. The  $K_D$  values were determined using Nano Temper software (NanoTemper Technologies).

### 2.9. Statistics

Statistical analyses were conducted using GraphPad Prism 10 software (GraphPad Software Inc., San Diego, CA). For the cellular functional assays including real-time PCR analysis, Caspase 3/7-mediated apoptosis assay, and Western blot analysis, the experiments were repeated at least three times. Data were normalized with the unstimulated controls, and are expressed as the mean  $\pm$  standard error of mean (SEM). A significant difference was determined by ordinary one-way analysis of variance (ANOVA) followed by Dunnett's *post-hoc* test and multiple comparison test.  $P < 0.05$  was considered significant. P values generated during the statistical analyses were summarized in the supplementary datasheet.

## 3. Results

### 3.1. Network pharmacology revealed quercetin, luteolin, kaempferol, morin, and $\beta$ -sitosterol as key components in PV for treating HT

The currently identified components of PV were obtained from the TCMSP database and subsequent network pharmacology [8]. Two parameters,  $DL \geq 0.18$  and  $OB \geq 30\%$ , were used as criteria for screening [9]. As a result, 11 components of PV with component targets were retrieved (SupplementaryTable.1). On the other hand, over 3000 genes associated with HT (i.e. disease targets) were obtained from databases including GeneCards, OMIM, DrugBank, and PharmGKB (Fig. 1a). The intersection of the component targets and the disease targets: a total of 154 gene targets were then gathered as the potential targets of PV for HT (Fig. 1b). The 154 genes were imported into the STRING database to construct a PPI network (Fig. 1c), and subjected to KEGG pathway enrichment to draw potential signaling pathways underlying the mechanisms of PV to treat HT (Fig. 1d). Accordingly, a network of component-target interactions containing 203 nodes (11 components and 192 targets including 154 HT-related targets) was established (Fig. 1e). To further screen key components of PV and their targets; the centrality degree of each node in both component-target interaction network and the PPI network was calculated. After two rounds of screening based on centrality degree, four flavonoids including quercetin, luteolin, kaempferol, morin, and a phytosterol,  $\beta$ -sitosterol were left as key components in PV for HT (Fig. 1e). And the key targets include HSP90AA1, TNF- $\alpha$ , Caspase 3 (CASP3), transcription factor 65 (RELA/p65), peroxisome proliferator activated receptor gamma (PPARG), RAC-alpha serine/threonine-protein kinase 1 (AKT1), transcription factor Jun (JUN) (Fig. 1e). We next tested whether the key components could reproduce the innate immune-modulating and anti-apoptosis activities of PV in stimulated human thyrocytes.



### 3.2. *PV* components suppressed gene expressions of inflammatory cytokines induced by dsDNA/dsRNA in primary human thyrocytes and Nthy-ori-31 cells

We previously showed that aqueous *PV* extracts abolished gene expressions of inflammatory cytokines induced by dsDNA or dsRNA in rat thyroid FRTL-5 cells [7]. Herein we tested whether the key components of *PV* could reproduce such an anti-inflammatory effect of *PV* in stimulated human thyrocytes. Primary human thyrocytes were derived from non-cancerous thyroid tissues during thyroid surgery. Consistent with the previous study in FRTL-5 cells [7], stimulation with either dsDNA (Fig. 2a) or dsRNA (Fig. 2b) activated an innate immune response in primary human thyrocytes, as shown by the skyscraping expressions of *TNF $\alpha$* , *IFN $\beta$ 1*, and *IL6* in cells, though the extent of inflammatory gene inductions could vary among the donors. Each *PV* component, quercetin, luteolin, kaempferol, morin or  $\beta$ -sitosterol, was given in the stimulated cells at two doses without observed cytotoxic effects. Inhibition of inflammatory cytokine genes was observed for each *PV* component in a dose-dependent manner (Fig. 2). Similar anti-inflammatory effects of key *PV* components were also confirmed in a human thyroid cell line, Nthy-ori-31 cells. Stimulation with either dsDNA (Fig. 3a) or dsRNA (Fig. 3b) induced gene expressions of *TNF $\alpha$* , *IFN $\beta$ 1*, and *IL6* in Nthy-ori-31 cells, which was inhibited by the treatment of each *PV* component dose-dependently (Fig. 3). The predicted key *PV* components could thus reproduce an anti-inflammatory effect of *PV* to inhibit gene expressions of pro-inflammatory cytokines in stimulated human thyrocytes.

### 3.3. *PV* components suppressed Caspase 3/7-mediated apoptosis induced by dsDNA/dsRNA in human thyrocytes

We previously showed that either dsDNA or dsRNA induced significant cell death in FRTL-5 cells, which was abolished by aqueous *PV* extracts [7]. We then tested whether the *PV* components could reproduce such an anti-apoptosis effect of *PV* in stimulated human thyrocytes. Caspase 3/7 belongs to the Caspase family [13]. Caspase 3/7 plays a key role in the process of nuclear apoptosis, including chromatin condensation and DNA fragmentation [13]. Caspase 3/7 also plays a crucial role in cell blebbing apoptosis [14]. Thus live-cell analysis continuously monitored cells undergoing Caspase 3/7-mediated apoptosis for over 24 h after dsDNA/dsRNA stimulation. The results showed that the Caspase 3/7-mediated apoptosis continuously increased in Nthy-ori-31 cells after the stimulation with dsDNA (Fig. 4a and b) or dsRNA (Fig. 5a and b) throughout the observation period, which was significantly suppressed by each *PV* component dose-dependently to different extents (Figs. 4 and 5).

### 3.4. *PV* components inhibited the expressions of phosphorylated IRF-3 (pIRF-3) and phosphorylated inhibitor $\kappa$ B- $\alpha$ (pI $\kappa$ B- $\alpha$ ) in stimulated human thyrocytes

We previously showed that in stimulated FRTL-5 cells aqueous *PV* extracts inhibited the transactivation of transcription factors IRF-3 and NF- $\kappa$ B by suppressing the protein expression of pIRF-3 and interfering with the protein degradation of I $\kappa$ B- $\alpha$ , respectively [7]. IRF-3 and NF- $\kappa$ B are major regulators in innate immune response and inflammation [15,16]. In non-stimulated cells, IRF-3 is in an inactive cytoplasmic form. Upon stimulations, IRF-3 is phosphorylated at serine/threonine, allowing its nuclear translocation to activate the transcription of type I IFNs and IFN-inducible genes [15]. Similarly, in non-stimulated cells, NF- $\kappa$ B is also in an inactive cytoplasmic form sequestered by a family of inhibitors, termed inhibitors of  $\kappa$ B (I $\kappa$ B). Upon stimulations, I $\kappa$ B proteins are phosphorylated followed by degradation, thus freeing NF- $\kappa$ B for its further activation [16]. To investigate whether the predicted *PV* components also regulate the activation of IRF-3 or NF- $\kappa$ B in stimulated human thyrocytes, we examined the phosphorylated protein levels of IRF-3 and I $\kappa$ B- $\alpha$  (the major subtype of I $\kappa$ B) by Western blot analysis. Thus, Nthy-ori-31 cells were stimulated with dsDNA or dsRNA in the presence or absence of each *PV* component for 6 h. In non-stimulated cells, either pIRF-3 or pI $\kappa$ B- $\alpha$  was hardly detectable (Fig. 6a). At 6 h after the stimulation with either dsDNA or dsRNA substantial protein expressions of pIRF-3 and pI $\kappa$ B- $\alpha$  were detected (Fig. 6a), indicating the activation of IRF-3 and NF- $\kappa$ B, respectively. The induction of pIRF-3 and pI $\kappa$ B- $\alpha$  was not significantly affected by the vehicle of DMSO or EtOH, but inhibited by the treatment with each *PV* component in a dose-dependent manner (Fig. 6a and b). Thus, the *PV* components reproduced a suppressing effect of *PV* on the transactivation of IRF-3 and NF- $\kappa$ B.

### 3.5. HSP90AA1 was identified as an interacting protein with the flavonoid components of *PV* in inflamed primary human thyrocytes

To explore the proteins that interact with flavonoid components of *PV* in inflamed human thyrocytes, chemical proteomics screening following a Lip-MS workflow was performed in inflamed primary human thyrocytes. Luteolin, morin, quercetin, or the vehicle DMSO at the same concentration was each incubated with the same amount of total proteins extracted from dsDNA/dsRNA-stimulated primary human thyrocytes, followed by Lip-MS workflow (Fig. 7a). The strategy is based on the fact that proteins are more stable when bound with a small molecule, which makes them more resistant to proteolysis [17]. Protein lysates were compared in the presence and absence of a flavonoid (luteolin, morin, or quercetin). Proteins that bind to small molecules are protected from proteolysis relative to the control (DMSO-incubated samples), as revealed by mass spectrometry (Fig. 7a). Lip-MS identified 380 proteins interacting with all three flavonoids (Fig. 7b and c), out of which 9 are also potential *PV* targets for HT as revealed by network pharmacology (Fig. 7d), including HSP90AA1, heat shock protein A5 (HSPA5), intercellular adhesion molecule-1(ICAM1), NAD(P)H quinine dehydrogenase 1 (NQO1), aldo-keto reductase family 1 member B (AKR1B1), superoxide dismutase 1 (SOD1), cyclin-dependent kinase 1 (CDK1), poly (ADP-ribose) polymerase 1 (PARP1), glutathione S-transferase P1 (GSTP1). In particular, HSP90AA1 was revealed as a key target common for quercetin, luteolin, kaempferol, morin, and  $\beta$ -sitosterol to treat HT by network pharmacology (Fig. 1e). To verify the direct interactions between HSP90AA1 and the key *PV* components, microscale thermophoresis binding assays were performed to determine their binding affinities i.e.  $K_D$  values. The results showed that morin had the highest

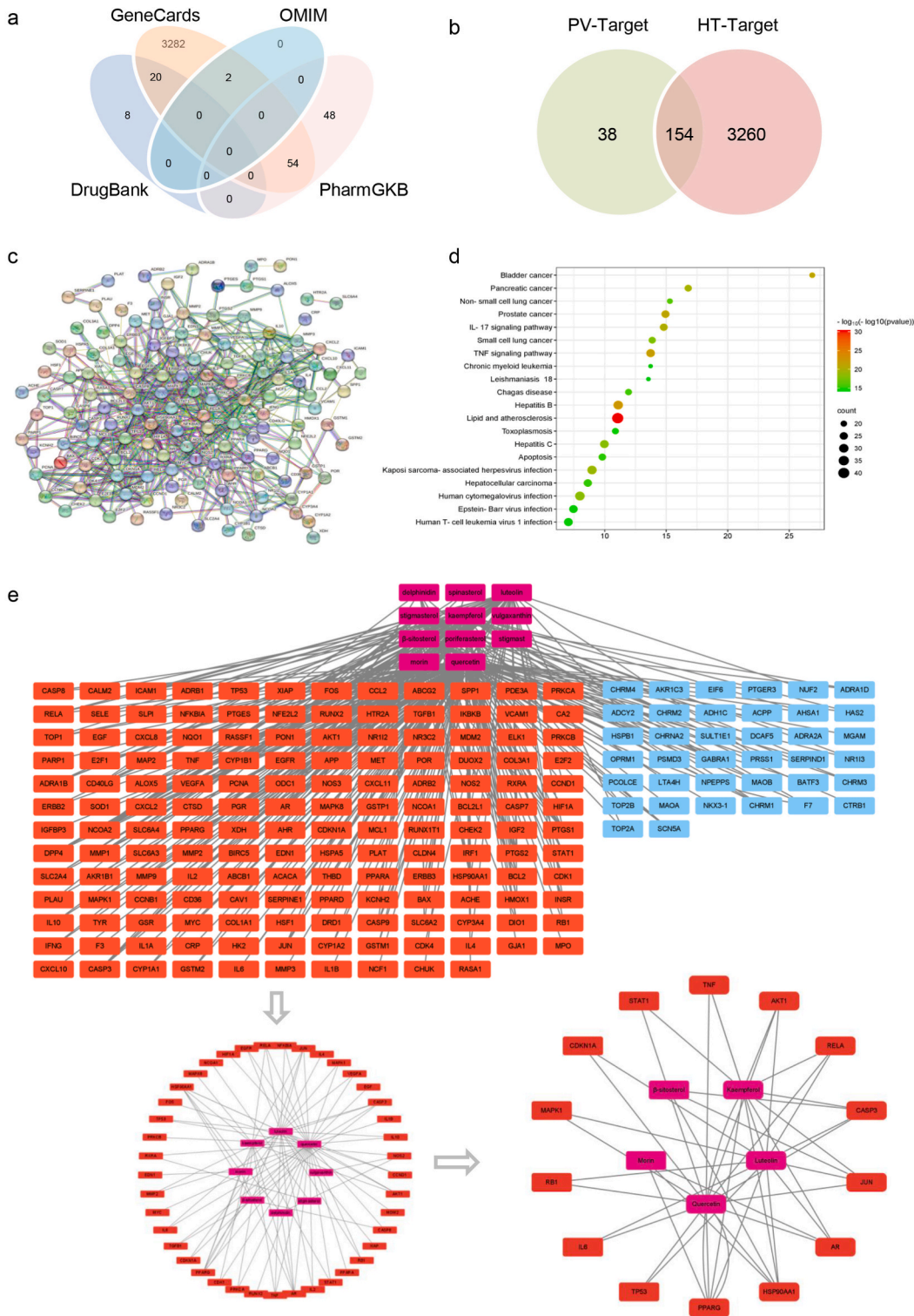


**Fig. 1.** Network pharmacology of PV components and targets for HT (a) The Venn diagram showing disease targets of HT obtained from four databases including GeneCards, OMIM, DrugBank, and PharmGKB. (b) The Venn diagram shows the intersection between the targets of PV and HT: a total of 154 gene targets were obtained as the potential targets of PV to treat HT. (c) The 154 genes were imported into the STRING database to construct a PPI network. (d) The 154 genes were subjected to KEGG pathway enrichment analysis. The top 20 signaling pathways were shown. (e) The 11 violet nodes on the top represent bioactive PV components with DL > 0.18 and OB > 30 %; the 192 (red and blue) nodes at below represent targets of the components, among which 154 red nodes are also disease targets associated with HT. The grey edges represent the interactions

between the nodes. The centrality degree value was used as a reference for the importance of a node. A component-target network containing 8 *PV* components (violet) and 41 targets (red) was obtained after the first round of screening by CytoNCA. A core component-target network containing 5 *PV* components (violet) and 14 targets (red) was obtained after the second round of screening by CytoNCA.

affinity with HSP90AA1 ( $K_D = 122.74 \mu\text{M}$ ) (Fig. 8a), followed by kaempferol ( $K_D = 168.53 \mu\text{M}$ ) (Fig. 8b), luteolin ( $K_D = 293.94 \mu\text{M}$ ) (Fig. 8c), and quercetin ( $K_D = 356.86 \mu\text{M}$ ) (Fig. 8d), while  $\beta$ -sitosterol showed no affinity with HSP90AA1 (Fig. 8e). Molecular docking was accordingly performed to visualize predicted interactions between HSP90AA1 and the four flavonoid components of *PV* (Supplementary Fig. 1).

#### 4. Discussion

As the precise pathogenesis of HT remains unclear, currently there is no effective way to treat HT. The management of HT is mainly the control of hypothyroidism. While hypothyroidism is treated with L-T4, the thyroid inflammation and destruction in HT are left untreated. Some euthyroid patients with HT continue to experience persisting symptoms or lower quality of life, putatively due to the ongoing thyroid autoimmune process [18]. The herbal medicine *PV* provides a natural remedy for HT.

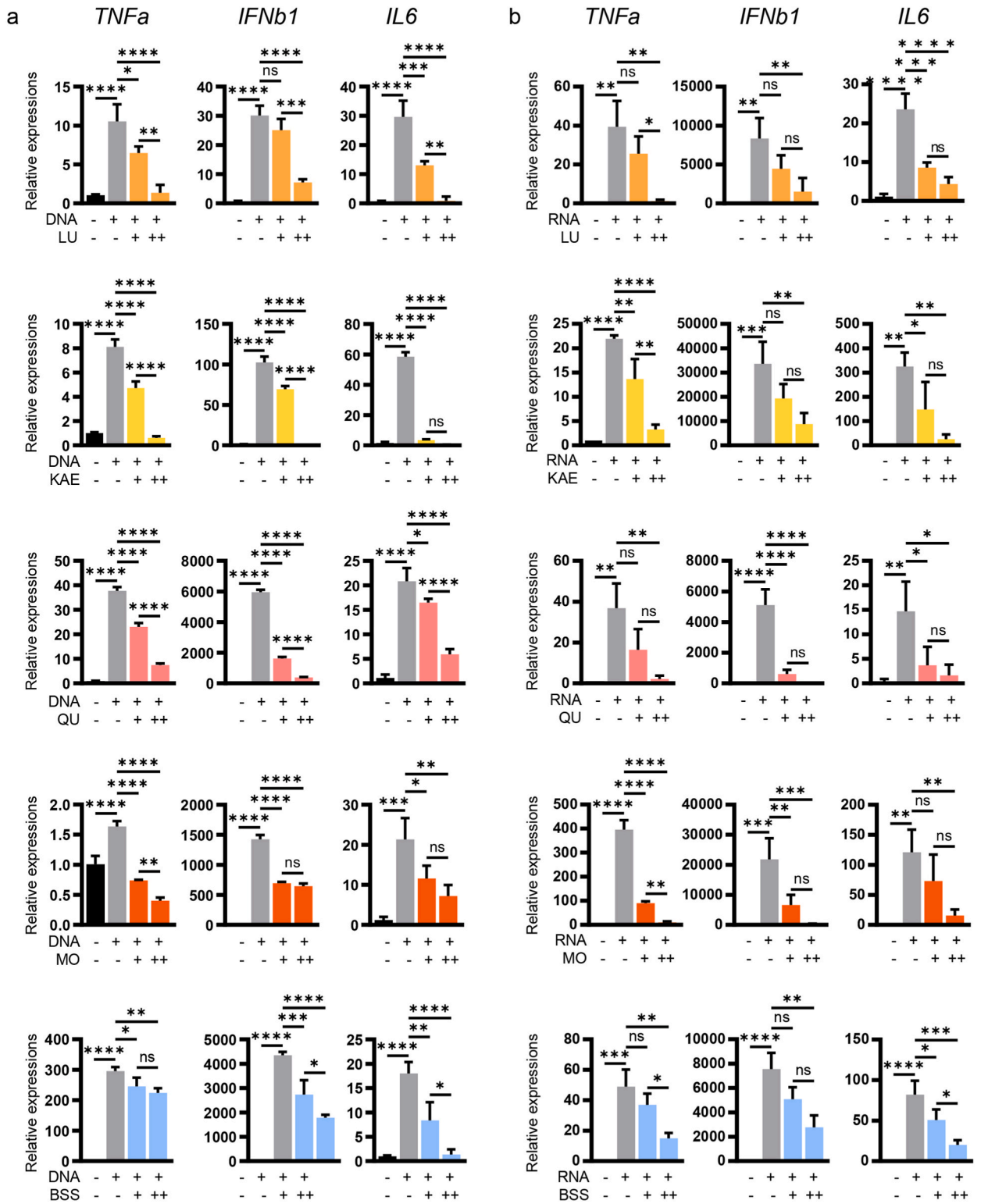
*PV* is called an “all-healing” plant with antioxidant, anti-allergic, anti-inflammatory, and antimicrobial activities [19]. *PV* is approved to treat sore throats, intestinal infections, diarrhea, migraine, fever and etc. in Europe and Asia [19]. For thyroid dysfunctions, *PV* has a great scientific interest and practical use. *PV* in combination with L-T4 has better clinical efficiency in treating patients with HT [6], as the combination therapy with *PV* further reduced the diameter of thyroid nodules, the autoantibody (TPO-Ab and TG-Ab) titers, and the proportions of T helper 17 (Th17) cells in HT [6,20].

To screen the core bioactive components of *PV* for HT treatment, we employed the methods of network pharmacology. Network pharmacology is a rational approach to studying traditional herbal medicines, which is effective for establishing a ‘component-target-disease’ network and revealing the regulation mechanisms of small molecules in a high-throughput manner. As a result, quercetin, luteolin, kaempferol, morin, and  $\beta$ -sitosterol are predicted as key components in *PV* to treat HT.

Quercetin, luteolin, kaempferol, and morin belong to a family of flavonoids [21]. They share homologous molecular structures and exert anti-inflammatory activities through several mechanisms such as by scavenging reactive oxygen and nitrogen species (ROS and RNS) formed in the cells [22]; by inhibiting the production of inflammatory mediator-producing enzymes including cyclooxygenase (COX) and lipoxygenase (LOX) [23]; by reducing the production of pro-inflammatory mediators like TNF- $\alpha$ , IL-1 $\beta$ , IL-6, IL-8, nitric oxide (NO) [24]; by modulating expression and phosphorylation of protein kinases involved in inflammatory signal cascades like mitogen activated protein kinase (MAPK), protein kinase C (PKC), phosphatidylinositol 3-kinases (PI3K), extracellular signal-regulated kinase (ERK), c-Jun N-terminal kinase (JNK) [25]; by disturbing transactivation of transcription factors including NF- $\kappa$ B, activator protein-1 (AP1), signal transducer and activator of transcription 3 (STAT3), nuclear factor 2 (NRF2) [26,27]; by inhibiting the expressions of endothelial adhesion molecules like ICAM-1, vascular cell adhesion molecule-1 (VCAM1), selectins, integrins, monocyte chemoattractant protein-1 (MCP1) [28]; by regulating matrix metalloproteinases (MMP) and tissue inhibitors of metalloproteinases (TIMP) [29]. Anti-inflammatory activities of quercetin, luteolin, kaempferol, or morin have been demonstrated in a large panel of cell types including both immune cells (such as macrophages, monocytes, neutrophils, T cells, and mast cells) and non-immune cells (such as liver cells, pulmonary cells, renal cells, epidermal cells, cancer cells) [21]. Flavonoids are therefore potential therapeutic candidates in various inflammatory and autoimmune disorders such as acute necrotizing pancreatitis [30], arthritis [31], mastitis [32], diabetes [33], Parkinson’s disease [34], and chronic asthma [35]. Meanwhile,  $\beta$ -sitosterol is a phytosterol with structural similarity to cholesterol and a broad spectrum of anti-inflammatory properties against various chronic illnesses [36]. Despite extensive studies of the five molecules, their acting mechanisms in HT had rarely been documented.

It has been suggested that activation of an innate immune response in thyrocytes facilitates autoimmunization, as a potential trigger for thyroid autoimmunity [2]. PAMP and DAMP are the two main patterns to induce an innate immune response and inflammation in cells. The former refers to exogenous molecules associated with pathogens (such as viral dsRNA), and the latter refers to endogenous molecules derived from damaged cells (such as self dsDNA). In the thyroid the PAMP- or DAMP-triggered innate immune response potentially sensitizes the adaptive immune system to respond to self-antigens by recruiting lymphocytes into local, expanding antigen presentations, and perturbing hormone synthesis in thyrocytes [2]. The inflammatory mediators released from thyrocytes along with the infiltrating lymphocytes might form *de novo* lymph follicles and transform the thyroid into an organ prone to autoimmunity [2]. We previously showed that dsDNA and dsRNA, representative of DAMP and PAMP respectively, induced a strong innate immune response in rat thyrocytes characterized by increased gene expressions of inflammatory cytokines and cell death, which was abolished by the treatment of aqueous *PV* extracts [7].

In the current study, we therefore tested whether the predicted key *PV* components for HT could reproduce such an innate immunomodulating and anti-apoptotic activity in stimulated human thyrocytes, which potentially contribute to the clinical efficacy of *PV* in HT. In line with the previous results [7], dsDNA/dsRNA induced an innate immune response with sharply increased gene expressions of inflammatory cytokines and visible cell death in primary human thyrocytes and Nthy-ori-31 cells. Each *PV* component, quercetin, luteolin, kaempferol, morin, and  $\beta$ -sitosterol, was administered to the stimulated cells at two doses. As expected, each *PV* component suppressed gene expressions of the inflammatory cytokines including TNF- $\alpha$ , IFN- $\beta$ , IL-6 in a dose-dependent manner in stimulated human thyrocytes. TNF- $\alpha$  and IL-6 are predicted key disease targets of *PV* for HT as indicated by network pharmacology, and KEGG pathway enrichment analysis also revealed that the TNF signaling pathway is potentially a key target of *PV* to treat HT (Supplementary Fig. 2a). Binding of TNF- $\alpha$  to its receptors on cell surface results in recruitment of signal transducers that activate at least three distinct



(caption on next page)



**Fig. 2.** PV components suppressed dsDNA/dsRNA-induced gene expressions of inflammatory cytokines in primary human thyrocytes Primary human thyrocytes were stimulated by dsDNA (a) or dsRNA (b) with or without treatment of PV components for 24 h. Unstimulated cells were used as a control, and data are presented as mean ± SEM (relative to the mRNA levels in unstimulated cells). LU: luteolin, KAE: kaempferol, QU: quercetin, MO: morin, BSS: β-sitosterol. For PV components, ‘+’ and ‘++’ indicate ‘low-dose’ and ‘high-dose’ treatment, respectively. A significant difference was determined by ordinary one-way ANOVA followed by Dunnet’s *post-hoc* test and multiple comparison test. \*: p < 0.05, \*\*: p < 0.01, \*\*\*: p < 0.001, \*\*\*\*: p < 0.0000.

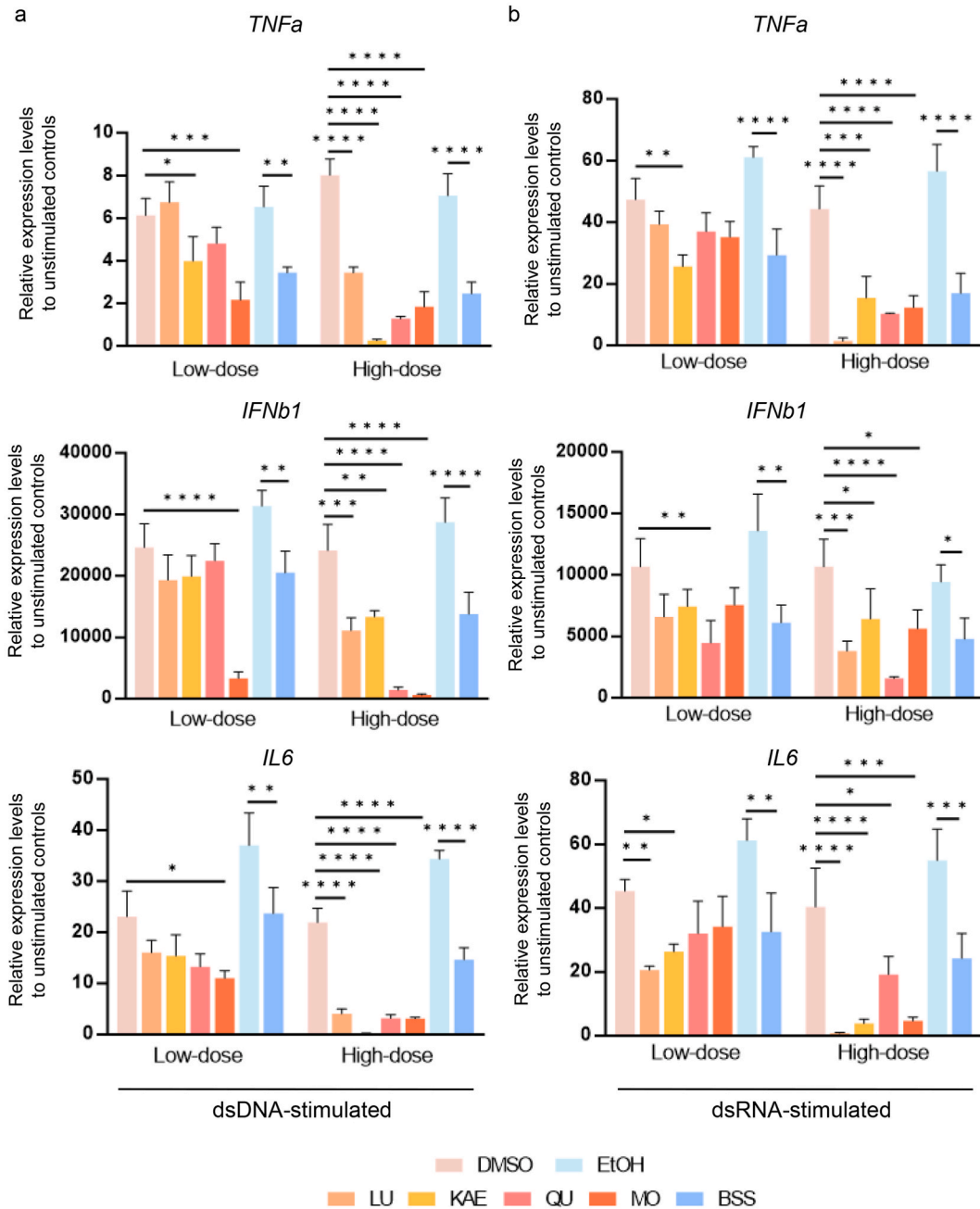


**Fig. 3.** PV components suppressed dsDNA/dsRNA-induced gene expressions of inflammatory cytokines in Nthy-ori-31 cells Nthy-ori-31 cells were stimulated by dsDNA (a) or dsRNA (b) with or without treatment of PV components/vehicles for 24 h. Unstimulated cells were used as a control, and data are presented as mean ± SEM (relative to the mRNA levels in unstimulated cells). LU: luteolin, KAE: kaempferol, QU: quercetin, MO: morin, BSS: β-sitosterol. A significant difference was determined by ordinary one-way ANOVA followed by Dunnet’s *post-hoc* test and multiple comparison test. \*: p < 0.05, \*\*: p < 0.01, \*\*\*: p < 0.001, \*\*\*\*: p < 0.0000.



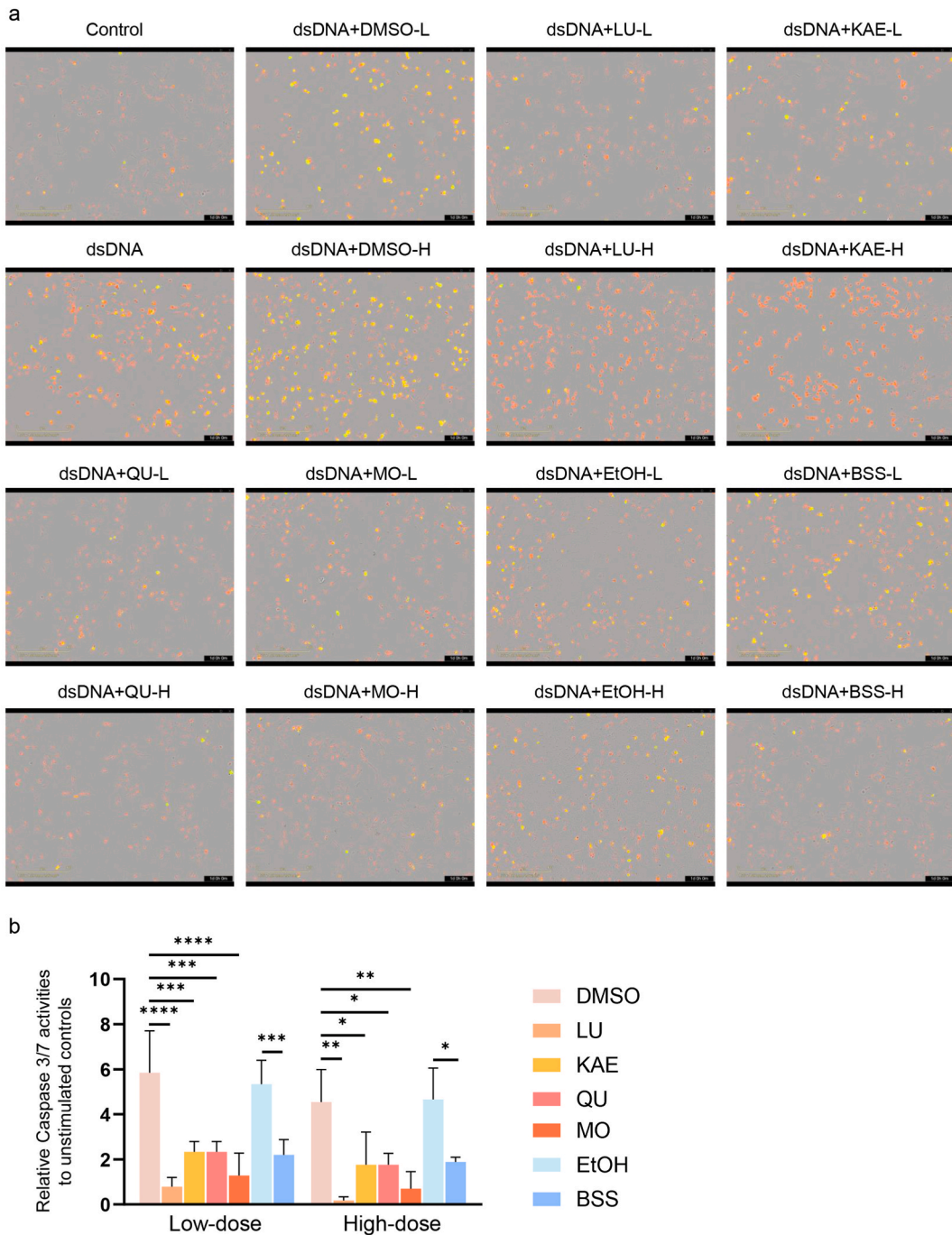


**Fig. 4.** PV components suppressed dsDNA-induced Caspase 3/7 activities in Nthy-ori-31 cells. Nthy-ori-31 cells were stimulated by dsDNA with or without treatment of PV components/vehicles for 24 h. (a) Live cells (red) and Caspase 3/7 activities (green) were monitored continuously for 24 h by live-cell imaging (full videos can be downloaded from [https://www.jianguoyun.com/p/DaT\\_Zn4Q2tfxChj98dkFIAA](https://www.jianguoyun.com/p/DaT_Zn4Q2tfxChj98dkFIAA)). LU: luteolin, KAE: kaempferol, QU: quercetin, MO: morin, BSS:  $\beta$ -sitosterol, L: low-dose, H: high-dose. (b) Unstimulated cells were used as a control, and data are presented as mean  $\pm$  SEM (relative to the Caspase 3/7 activities in unstimulated cells). A significant difference was determined by ordinary one-way ANOVA followed by Dunnett's *post-hoc* test and multiple comparison test. \*:  $p < 0.05$ , \*\*:  $p < 0.01$ , \*\*\*:  $p < 0.001$ , \*\*\*\*:  $p < 0.0000$ .

effectors [37]. These effectors lead to the activation of two transcription factors, AP-1 and NF- $\kappa$ B, and Caspases, and ultimately induce apoptosis [37]. It is reasonable to speculate that PV components act to suppress TNF- $\alpha$  released from inflamed thyrocytes to block the TNF signaling pathway, thus attenuating the following innate immune response and apoptosis.

To evaluate the potential anti-apoptosis activity of PV components, Caspase 3/7-mediated apoptosis was monitored for over 24 h in

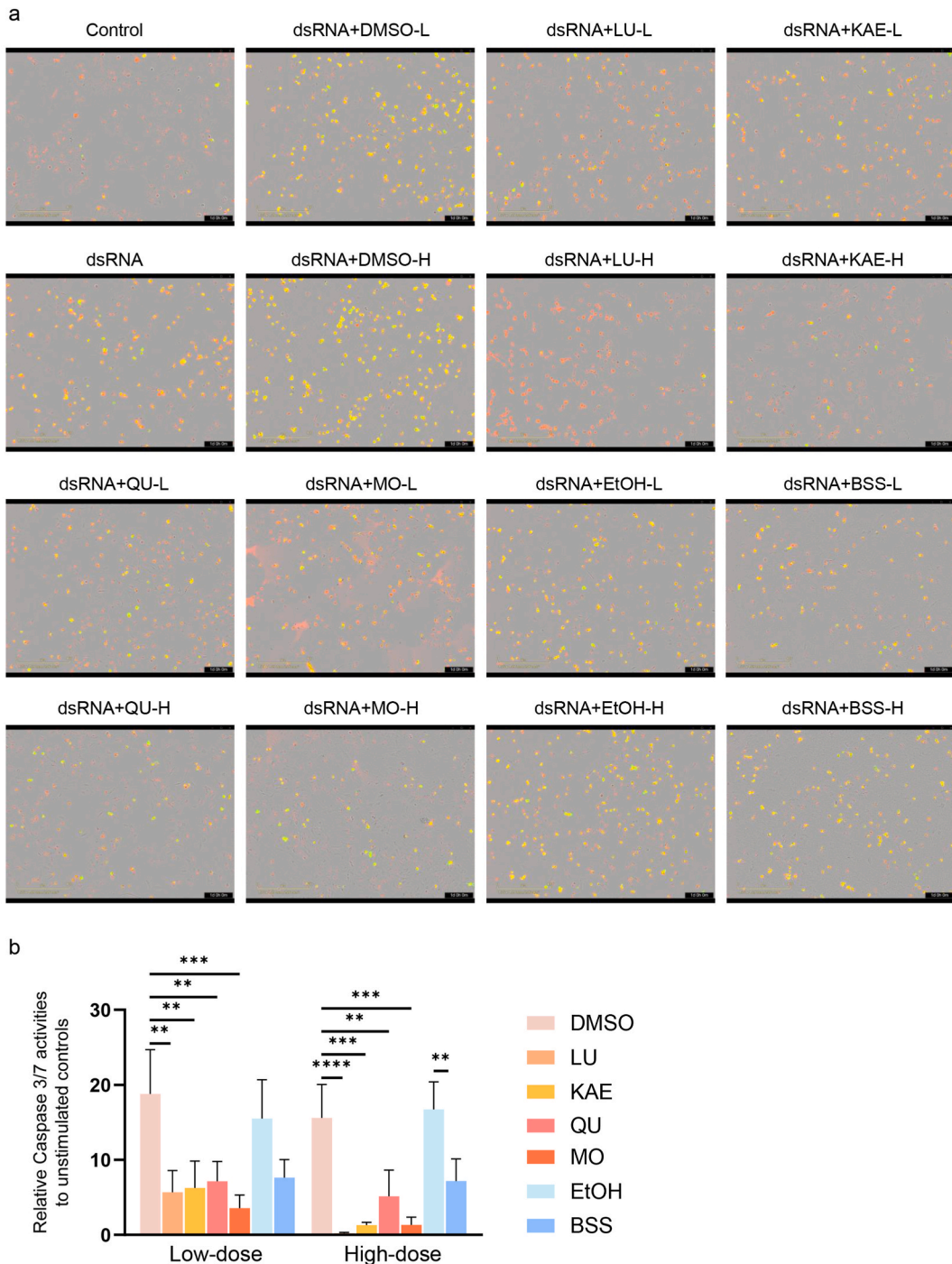


**Fig. 5.** PV components suppressed dsRNA-induced Caspase 3/7 activities in Nthy-ori-31 cells. Nthy-ori-31 cells were stimulated by dsRNA with or without treatment of PV components/vehicles for 24 h. (a) Live cells (red) and Caspase 3/7 activities (green) were monitored continuously for 24 h by live-cell imaging (full videos can be downloaded from [https://www.jianguoyun.com/p/DaT\\_Zn4Q2tfxChj98dkFIAA](https://www.jianguoyun.com/p/DaT_Zn4Q2tfxChj98dkFIAA)). LU: luteolin, KAE: kaempferol, QU: quercetin, MO: morin, BSS:  $\beta$ -sitosterol, L: low-dose, H: high-dose. (b) Unstimulated cells were used as a control, and data are presented as mean  $\pm$  SEM (relative to the Caspase 3/7 activities in unstimulated cells). A significant difference was determined by ordinary one-way ANOVA followed by Dunnett's *post-hoc* test and multiple comparison test. \*:  $p < 0.05$ , \*\*:  $p < 0.01$ , \*\*\*:  $p < 0.001$ , \*\*\*\*:  $p < 0.0000$ .

cells. The live-cell imaging pictured that Caspase 3/7-mediated apoptosis continuously increased throughout the observation period after dsDNA/dsRNA stimulation, which was suppressed by each PV component dose-dependently. The anti-apoptosis effect of PV components might be mediated through blocking the TNF signaling pathway as described above. It is also possible that PV targets

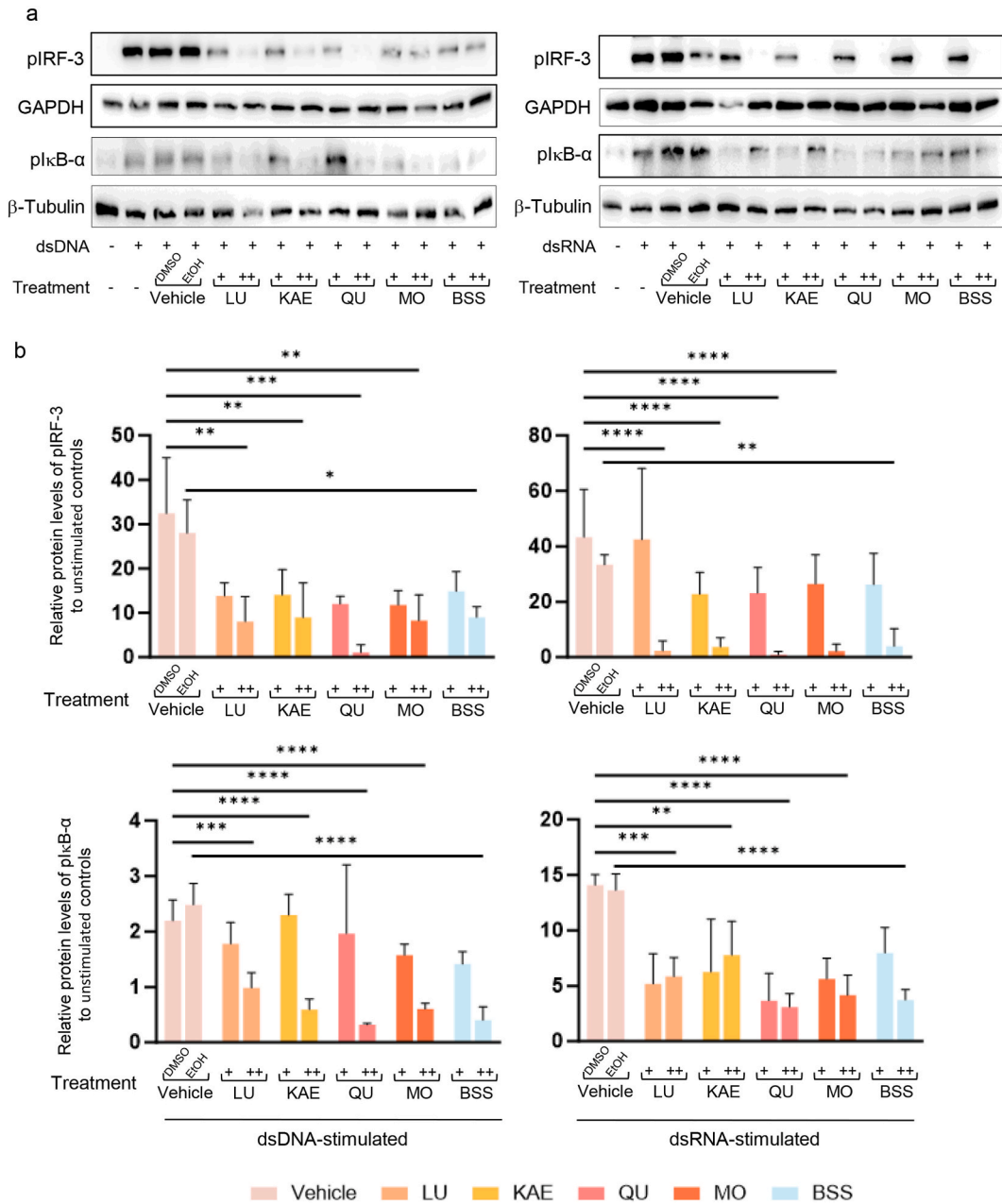


**Fig. 6.** PV components suppressed dsDNA/dsRNA-induced protein expressions of pIRF-3 and pIκB-α in Nthy-ori-31 cells. Nthy-ori-31 cells were stimulated by dsDNA/dsRNA with or without treatment of PV components/vehicles for 6 h. (a) Typical images of the Western blot analysis of pIRF-3, pIκB-α, GAPDH, and β-Tubulin. LU: luteolin, KAE: kaempferol, QU: quercetin, MO: morin, BSS: β-sitosterol. For PV components, ‘+’ and ‘++’ indicate ‘low-dose’ and ‘high-dose’ treatment respectively. Non-adjusted images were provided in Supplementary Fig. 3. (b) Grayscale values of each band was normalized with the reference bands GAPDH or β-Tubulin. Unstimulated cells were used as a control, and data are presented as mean ± SEM (relative to protein levels in unstimulated cells). A significant difference was determined by ordinary one-way ANOVA followed by Dunnett’s *post-hoc* test and multiple comparison test. \*:  $p < 0.05$ , \*\*:  $p < 0.01$ , \*\*\*:  $p < 0.001$ , \*\*\*\*:  $p < 0.0000$ .

several key molecules in the signaling pathway of apoptosis, such as Caspases *per se*, as indicated by network pharmacology (Supplementary Fig. 2b).

Furthermore, we showed that the treatment with each PV component significantly reduced protein levels of pIRF-3 and pIκB-α in dsDNA/dsRNA-stimulated Nthy-ori-31 cells, which is consistent with the effects of aqueous PV extracts in stimulated FRTL-5 cells [7]. Phosphorylation of IRF-3 and IκB-α are known as activating steps in transactivation of IRF-3 and NF-κB respectively that are essential in mediating innate immune responses and inflammation [15,16]. Thus, it is likely that PV components exert their innate immune-modulating effects by inhibiting the transactivation of IRF-3 and NF-κB in inflamed human thyrocytes. In agreement, IκB-α



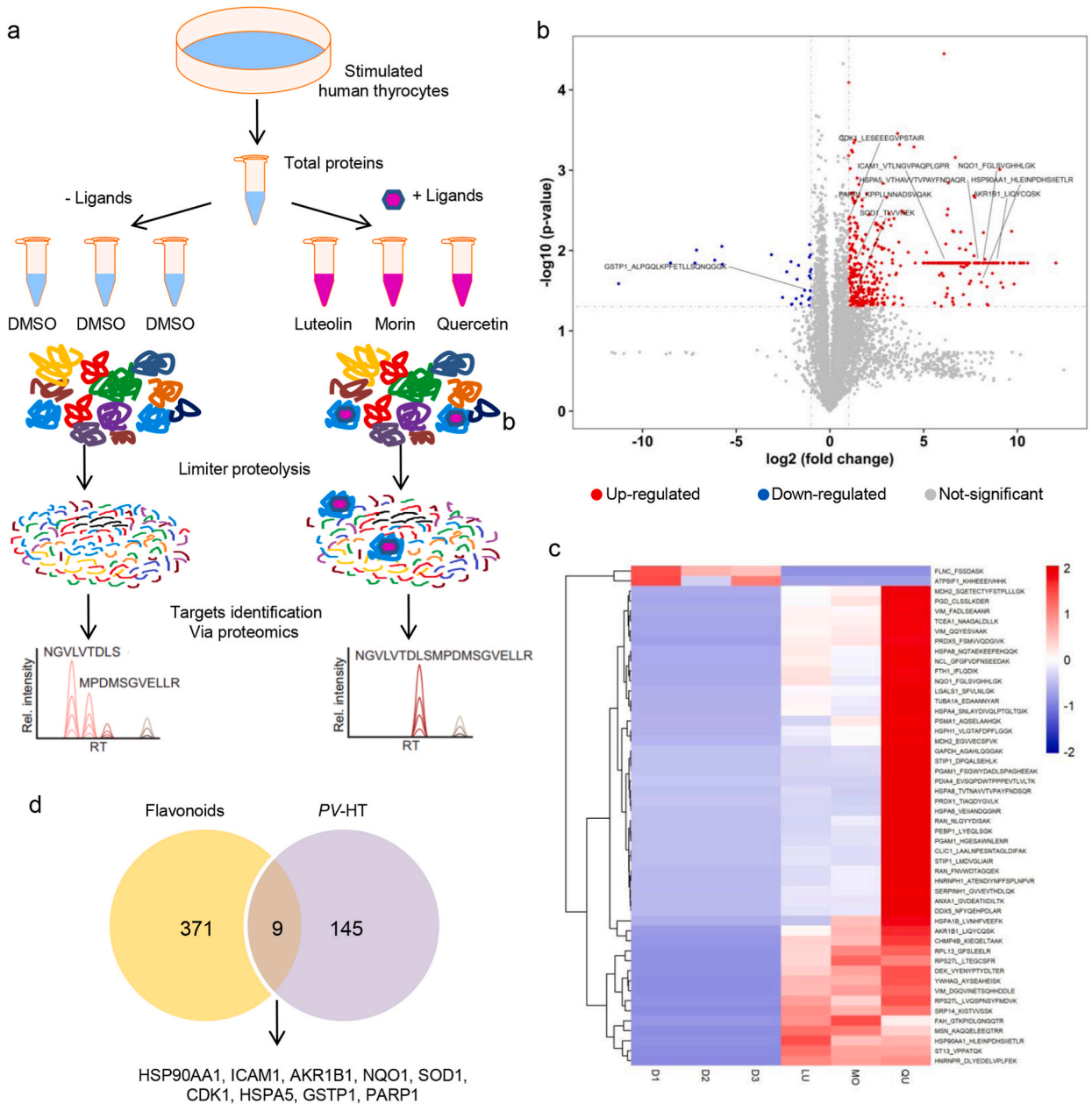


**Fig. 7.** Lip-MS identified proteins interacting with flavonoids in inflamed human thryocytes (a) Primary human thryocytes were stimulated with 1  $\mu$ g of dsDNA/dsRNA for 6 h. The stimulated cells were mixed up, and total proteins were extracted and aliquoted in 6 equivalent volumes. Luteolin, morin, quercetin, or the vehicle DMSO at the same concentration was each incubated with the same amount of total proteins extracted from the stimulated cells. Proteins bound to the small molecule are protected from proteolysis relative to the control (i.e. DMSO-incubated samples), as indicated by mass spectrometry. (b) Volcano plots showed interacting proteins of all three flavonoids, luteolin, morin, and quercetin, as identified by Lip-MS. Fold change (FC) > 2 or < 0.5,  $p < 0.05$  were read out as significant. (b) Heat-map of the top 50 interacting protein peptides with flavonoids as identified by Lip-MS experiments. D1, D2, D3: triplicates of DMSO-incubated samples; QU, LU, MO: quercetin/luteolin/morin-incubated samples. (c) Among the identified interacting proteins 380, nine including HSP90AA1, ICAM1, AKR1B1, NQO1, SOD1, CDK1, HSPA5, GSTP1, andPARP1 were also predicted PV targets for HT as revealed by network pharmacology.

and RELA/p65 (a protein that forms NF- $\kappa$ B heterodimer) are also predicted targets of PV for HT (Supplementary Fig. 2c). With Lip-MS approach, we explored proteins directly interacting with flavonoid components of PV in inflamed primary human thryocytes. As a result, HSP90AA1 was identified as a common interacting protein target for quercetin, luteolin, and morin by Lip-MS. With microscale thermophoresis binding assay, the affinity of each PV component with HSP90AA1 was determined. The results confirmed that the four flavonoids (quercetin, luteolin, kaempferol, morin) have good binding affinities with HSP90AA1 ( $K_D$  values

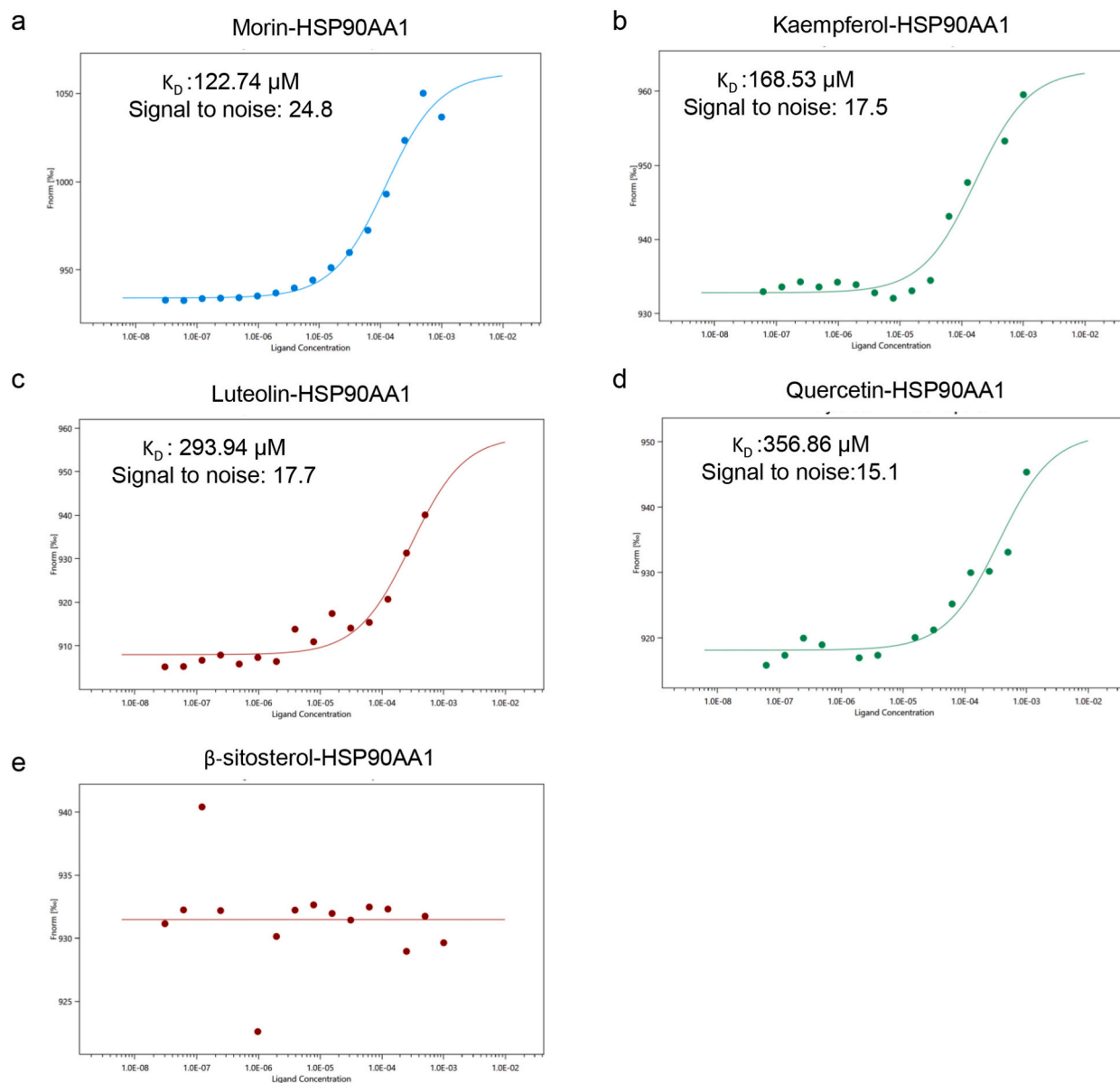


**Fig. 8.** Microscale thermophoresis binding assays for PV components with HSP90AA1 protein His-tag labeled human HSP90AA1 protein was incubated with serial diluted ligands/DMSO (30 nM up to 1 mM), and detected by the microthermophoresis. The  $K_D$  value and the signal-to-noise value were indicated for each potential ligand accordingly. Morin (a) had the highest affinity with HSP90AA1, followed by kaempferol (b), luteolin (c), and quercetin (d), while  $\beta$ -sitosterol (e) showed no affinity with HSP90AA1.

ranged from 122.74  $\mu$ M to 356.86  $\mu$ M), while  $\beta$ -sitosterol (up to 1 mM) showed no binding affinity with HSP90AA1. HSP90AA1 has been predicted as a key target of PV components for HT by our network pharmacology analysis. Anti-HSP90 therapy has been attempted in preclinical studies of autoimmune and inflammatory diseases such as rheumatoid arthritis, systemic lupus erythematosus, encephalomyelitis and etc. [38]. The underlying mechanism responsible for the immunoregulatory effects of HSP90 inhibition remains inconclusive. One theory has linked the immunoregulatory effect of HSP90 inhibitors to HSP90-dependent activation of NF- $\kappa$ B [38]. Others speculate that the anti-inflammatory effects of HSP90 inhibitors are mediated through heat shock factor 1 (HSF1), which drives gene expressions of anti-inflammatory molecules including IL-10 and HSP70 [38]. Thus, the flavonoids in PV may act as natural HSP90 inhibitors to suppress NF- $\kappa$ B-mediated inflammation while promoting HSF1-mediated anti-inflammatory process, thus protecting thyrocytes from inflammatory injuries in HT (Fig. 9).

There are several limitations in this study. Network pharmacology is based on database research, yet the database for traditional Chinese medicine is not perfect. There were 3414 disease targets of HT while only 192 drug targets of PV were retrieved from databases, thus the intersection of drug targets and disease targets was inevitably imbalanced in their respective proportions. Secondly,



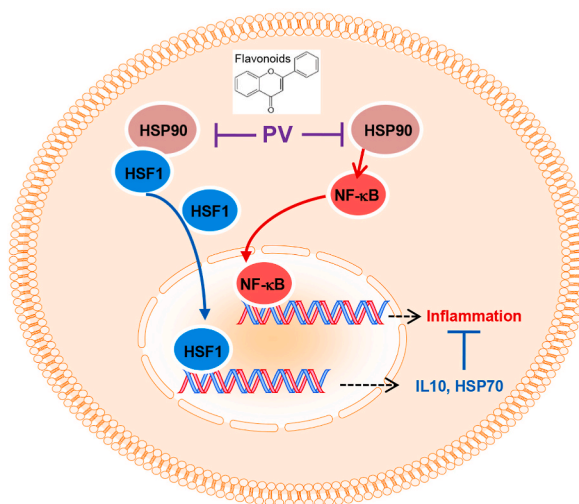


**Fig. 9.** Schematic representation of possible anti-inflammatory effects of PV as a natural HSP90 inhibitor in thyrocytes. Two opponent pathways are mediated through HSP90 in cells. HSP90 activates NF- $\kappa$ B-mediated inflammation. On the other hand, HSP90 associates with HSF1 to inactivate HSF1-mediated anti-inflammation. PV containing various flavonoids potentially acts as a natural HSP90 inhibitor, which suppresses NF- $\kappa$ B-mediated inflammation while promoting the disassociation of HSF1 and the following expressions of anti-inflammatory mediators such as IL-10, and HSP70.

the effectiveness of drugs is based on the active substances, which must reach a certain concentration to take effect. However, the plasma and tissue concentrations of PV components are unclear, and using them as the main pharmacological components of PV may only have theoretical significance. Also, different Chinese medicine preparations (e.g. different decoction methods) can affect the drug efficacy. Therefore, the components of PV in clinical practice can only be more complex than those in the database. We also notice that studies using network pharmacology to screen active ingredients of different drugs or prescriptions could obtain results with high similarity: flavonoids are among the most often reported compounds [9,39,40], potentially due to the inherent bias in the database research. Apart from the imperfection of network pharmacology, the validation experiments in this study were only on *in vitro* level, using primary human thyrocytes and a human thyroid follicular epithelial cell line, Nthy-ori-31 cells [41]. Primary human thyrocytes showed significant individual differences and were difficult to main differentiated *ex vivo*; while the use of Nthy-ori-31 cells is not welcomed by some, as its thyroid-specificity is less established than FRTL-5 cells (though the latter is not human-derived). There may be no perfect thyroid cells to use, nevertheless, our results obtained in primary human thyrocytes and Nthy-ori-31 cells were in agreement, which was also consistent with findings in the FRTL-5 cells [7]. For future validations, the three-dimensional culture of primary human thyrocytes [11], thyroid organoids, or experimental thyroid autoimmune animals are worth trying. Our findings have also raised a few interesting questions for future research: where are the binding sites of HSP90AA1 with flavonoids and what is the biological consequence of their interactions; whether HSP90AA1 play a role in thyroid inflammation and thus serving as a new therapeutic target; whether flavonoids affect adaptive immunity in thyroid cells which is an insurmountable step towards thyroid autoimmunity; and how flavonoids affect the immune cell function (e.g. Th17) in HT patients, given that the drug targets of PV were significantly enriched in the IL-17 signaling pathway. Low bioavailability is a major obstacle for flavonoids to be used as therapeutic agents, due to their lipophilic nature, lack of tissue-specificity, and rapid elimination [42]. To increase their plasma and tissue concentrations for the desired pharmacological effects, the development of tissue-targeting flavonoid delivery systems should be merited.

## 5. Conclusions

Quercetin, luteolin, kaempferol, morin, and  $\beta$ -sitosterol, predicted key PV components for HT in network pharmacology, reproduced an anti-inflammatory and anti-apoptosis effect of PV in stimulated human thyrocytes, which was likely, mediated via targets including HSP90AA1 and potentially underlying the beneficial effects of PV on HT.

## Ethics approval and consent to participate

Human thyroid tissues were obtained at the surgery with written consent. This study was performed in line with the principles of the Declaration of Helsinki. Approval was granted by the Ethical Committee of the institutional review boards of Nanjing Drum Tower Hospital, Nanjing, China (No.2021-601-02).

## Availability of data and materials

The authors confirm that the data supporting the findings of this study are available within the article (including the supplementary materials) and a public data repository ([https://www.jianguoyun.com/p/DaT\\_Zn4Q2tfxChj98dkFIAA](https://www.jianguoyun.com/p/DaT_Zn4Q2tfxChj98dkFIAA)), or can be made available from

the corresponding authors upon reasonable request.

## Funding

This work was supported by the National Natural Science Foundation of China (#81900712) and the Project of National Clinical Research Base of Traditional Chinese Medicine in Jiangsu Province, China (JD2023SZX12).

## CRediT authorship contribution statement

**Yongzhao Chen:** Writing – original draft, Methodology, Investigation. **Bo Jiang:** Writing – original draft, Visualization, Formal analysis, Data curation. **Cheng Qu:** Writing – original draft, Visualization, Validation, Software. **Chaoyu Jiang:** Writing – original draft, Formal analysis, Data curation. **Chen Zhang:** Writing – original draft, Resources. **Yanxue Wang:** Writing – original draft, Resources. **Fei Chen:** Writing – review & editing, Conceptualization. **Xitai Sun:** Writing – review & editing, Conceptualization. **Lei Su:** Writing – review & editing, Supervision, Conceptualization. **Yuqian Luo:** Writing – review & editing, Supervision, Funding acquisition, Conceptualization.

## Declaration of competing interest

The authors declare that they have no known competing financial interests or personal relationships that could have appeared to influence the work reported in this paper.

## Appendix A. Supplementary data

Supplementary data to this article can be found online at <https://doi.org/10.1016/j.heliyon.2024.e36103>.

## References

- [1] A.P. Weetman, An update on the pathogenesis of Hashimoto's thyroiditis, *J. Endocrinol. Invest.* 44 (5) (2021) 883–890, <https://doi.org/10.1007/s40618-020-01477-1>.
- [2] A. Kawashima, K. Yamazaki, T. Hara, T. Akama, A. Yoshihara, M. Sue, et al., Demonstration of innate immune responses in the thyroid gland: potential to sense danger and a possible trigger for autoimmune reactions, *Thyroid* 23 (4) (2013) 477–487, <https://doi.org/10.1089/thy.2011.0480>.
- [3] R.H. Mir, M.F. Bhat, G. Sawhney, P. Kumar, N.I. Andrabi, M. Shaikh, et al., *Prunella vulgaris* L: critical pharmacological, expository traditional uses and extensive phytochemistry: a review, *Curr. Drug Discov. Technol.* 19 (1) (2022) e140122191102, <https://doi.org/10.2174/1570163818666210203181542>.
- [4] W. Zhang, Q. Wuhan, M. Na, R. Hu, Q. Mu, X. Bao, Emerging therapeutic role of *Prunella vulgaris* in thyroid disease, *Chin Herb Med* 14 (3) (2022) 403–413, <https://doi.org/10.1016/j.chmed.2021.12.005>.
- [5] F. Li, Y. Wu, L. Chen, L. Hu, X. Liu, Initial treatment combined with *Prunella vulgaris* reduced prednisolone consumption for patients with subacute thyroiditis, *Ann. Transl. Med.* 7 (3) (2019) 45, <https://doi.org/10.21037/atm.2019.01.07>.
- [6] Q. Han, N. Xu, B. Chen, W. Wu, L. Sheng, Safety and efficacy of *Prunella vulgaris* preparation in adjuvant treatment of thyroid nodules: a meta-analysis, *Medicine (Baltim.)* 100 (41) (2021) e27490, <https://doi.org/10.1097/MD.00000000000027490>.
- [7] F. Chen, A. Kawashima, Y. Luo, M. Kiriya, K. Suzuki, Innate immune-modulatory activity of *Prunella vulgaris* in thyrocytes functions as a potential mechanism for treating hashimoto's thyroiditis, *Front. Endocrinol.* 11 (2020) 579648, <https://doi.org/10.3389/fendo.2020.579648>.
- [8] J. Ru, P. Li, J. Wang, W. Zhou, B. Li, C. Huang, et al., TCMSP: a database of systems pharmacology for drug discovery from herbal medicines, *J. Cheminform* 6 (2014) 13, <https://doi.org/10.1186/1758-2946-6-13>.
- [9] X.X. Gan, L.K. Zhong, F. Shen, J.H. Feng, Y.Y. Li, S.J. Li, et al., Network pharmacology to explore the molecular mechanisms of *Prunella vulgaris* for treating hashimoto's thyroiditis, *Front. Pharmacol.* 12 (2021) 700896, <https://doi.org/10.3389/fphar.2021.700896>.
- [10] P. Shannon, A. Markiel, O. Ozier, N.S. Baliga, J.T. Wang, D. Ramage, et al., Cytoscape: a software environment for integrated models of biomolecular interaction networks, *Genome Res.* 13 (11) (2003) 2498–2504, <https://doi.org/10.1101/gr.1239303>.
- [11] B. Jiang, C. Wang, C. Qu, C. Jiang, C. Zhang, Y. Chen, et al., Primary human thyrocytes maintained the function of thyroid hormone production and secretion in vitro, *J. Endocrinol. Invest.* 46 (12) (2023) 2501–2512, <https://doi.org/10.1007/s40618-023-02103-6>.
- [12] L. Zhang, L. Jiang, L. Yu, Q. Li, X. Tian, J. He, et al., Inhibition of UBA6 by inosine augments tumour immunogenicity and responses, *Nat. Commun.* 13 (1) (2022) 5413, <https://doi.org/10.1038/s41467-022-33116-z>.
- [13] S.A. Lakhani, A. Masud, K. Kuida, G.A. Porter Jr., C.J. Booth, W.Z. Mehal, et al., Caspases 3 and 7: key mediators of mitochondrial events of apoptosis, *Science* 311 (5762) (2006) 847–851, <https://doi.org/10.1126/science.1115035>.
- [14] M. Sebbagh, C. Renvoize, J. Hamelin, N. Riche, J. Bertoglio, J. Breard, Caspase-3-mediated cleavage of ROCK 1 induces MLC phosphorylation and apoptotic membrane blebbing, *Nat. Cell Biol.* 3 (4) (2001) 346–352, <https://doi.org/10.1038/35070019>.
- [15] C.A. Jefferies, Regulating IRFs in IFN driven disease, *Front. Immunol.* 10 (2019) 325, <https://doi.org/10.3389/fimmu.2019.00325>.
- [16] T. Liu, L. Zhang, D. Joo, S.C. Sun, NF-kappaB signaling in inflammation, *Signal Transduct Target Ther* 2 (2017) 17023, <https://doi.org/10.1038/sigtrans.2017.23>.
- [17] A. McFedries, A. Schwaib, A. Saghatelian, Methods for the elucidation of protein-small molecule interactions, *Chem Biol* 20 (5) (2013) 667–673, <https://doi.org/10.1016/j.chembiol.2013.04.008>.
- [18] K. Memeh, B. Ruhle, T. Vaghaiwalla, E. Kaplan, X. Keutgen, P. Angelos, Thyroidectomy for euthyroid patients with Hashimoto thyroiditis and persisting symptoms: a cost-effectiveness analysis, *Surgery* 169 (1) (2021) 7–13, <https://doi.org/10.1016/j.surg.2020.03.028>.
- [19] M.E. Zholdasbayev, G.A. Atazhanova, S. Musozoda, E. Poleszak, *Prunella vulgaris* L.: an updated overview of botany, chemical composition, extraction methods, and biological activities, *Pharmaceuticals* 16 (8) (2023), <https://doi.org/10.3390/ph16081106>.
- [20] Q. Guo, H. Qu, H. Zhang, X. Zhong, *Prunella vulgaris* L. Attenuates experimental autoimmune thyroiditis by inhibiting HMGB1/TLR9 signaling, *Drug Des Devel Ther* 15 (2021) 4559–4574, <https://doi.org/10.2147/DDDT.S325814>.
- [21] M. Chagas, M.D. Behrens, C.J. Moragas-Tellis, G.X.M. Penedo, A.R. Silva, C.F. Goncalves-de-Albuquerque, Flavonols and flavones as potential anti-inflammatory, antioxidant, and antibacterial compounds, *Oxid. Med. Cell. Longev.* 2022 (2022) 9966750, <https://doi.org/10.1155/2022/9966750>.

- [22] H. Speisky, F. Shahidi, A. Costa de Camargo, J. Fuentes, Revisiting the oxidation of flavonoids: loss, conservation or enhancement of their antioxidant properties, *Antioxidants* 11 (1) (2022), <https://doi.org/10.3390/antiox11010133>.
- [23] F. Gendrisch, P.R. Esser, C.M. Schempp, U. Wollfe, Luteolin as a modulator of skin aging and inflammation, *Biofactors* 47 (2) (2021) 170–180, <https://doi.org/10.1002/biof.1699>.
- [24] M. Jayachandran, Z. Wu, K. Ganesan, S. Khalid, S.M. Chung, B. Xu, Isoquercetin upregulates antioxidant genes, suppresses inflammatory cytokines and regulates AMPK pathway in streptozotocin-induced diabetic rats, *Chem. Biol. Interact.* 303 (2019) 62–69, <https://doi.org/10.1016/j.cbi.2019.02.017>.
- [25] S.C. Cheng, W.C. Huang, S.P. Jh, Y.H. Wu, C.Y. Cheng, Quercetin inhibits the production of IL-1 beta-induced inflammatory cytokines and chemokines in ARPE-19 cells via the MAPK and NF-kappaB signaling pathways, *Int. J. Mol. Sci.* 20 (12) (2019), <https://doi.org/10.3390/ijms20122957>.
- [26] Q. Ren, F. Guo, S. Tao, R. Huang, L. Ma, P. Fu, Flavonoid fisetin alleviates kidney inflammation and apoptosis via inhibiting Src-mediated NF-kappaB p65 and MAPK signaling pathways in septic AKI mice, *Biomed. Pharmacother.* 122 (2020) 109772, <https://doi.org/10.1016/j.biopha.2019.109772>.
- [27] M.M. Abdel-Fattah, W.R. Mohamed, E.H.M. Hassanein, H.A. Arab, E.A. Arafa, Role of NF-kappaB/ICAM-1, JAK/STAT-3, and apoptosis signaling in the anticancer effect of tangeretin against urethane-induced lung cancer in BALB/c mice, *Life Sci.* 325 (2023) 121749, <https://doi.org/10.1016/j.lfs.2023.121749>.
- [28] Q. Meng, L. Pu, Q. Lu, B. Wang, S. Li, B. Liu, et al., Morin hydrate inhibits atherosclerosis and LPS-induced endothelial cells inflammatory responses by modulating the NFkappaB signaling-mediated autophagy, *Int Immunopharmacol* 100 (2021) 108096, <https://doi.org/10.1016/j.intimp.2021.108096>.
- [29] A. Hilliard, P. Mendonca, T.D. Russell, K.F.A. Soliman, The protective effects of flavonoids in cataract formation through the activation of Nrf2 and the inhibition of MMP-9, *Nutrients* 12 (12) (2020), <https://doi.org/10.3390/nu12123651>.
- [30] Z. Junyuan, X. Hui, H. Chunlan, F. Junjie, M. Qixiang, L. Yingying, et al., Quercetin protects against intestinal barrier disruption and inflammation in acute necrotizing pancreatitis through TLR4/MyD88/p38 MAPK and ERS inhibition, *Pancreatology* 18 (7) (2018) 742–752, <https://doi.org/10.1016/j.pan.2018.08.001>.
- [31] A.M. Mahmoud, A.M. Sayed, O.S. Ahmed, M.M. Abdel-Daim, E.H.M. Hassanein, The role of flavonoids in inhibiting IL-6 and inflammatory arthritis, *Curr. Top. Med. Chem.* 22 (9) (2022) 746–768, <https://doi.org/10.2174/1568026622666220107105233>.
- [32] W.J. Sun, E.Y. Wu, G.Y. Zhang, B.C. Xu, X.G. Chen, K.Y. Hao, et al., Total flavonoids of *Abrus cantoniensis* inhibit CD14/TLR4/NF-kappaB/MAPK pathway expression and improve gut microbiota disorders to reduce lipopolysaccharide-induced mastitis in mice, *Front. Microbiol.* 13 (2022) 985529, <https://doi.org/10.3389/fmicb.2022.985529>.
- [33] G.R. Gandhi, A.B.S. Vasconcelos, D.T. Wu, H.B. Li, P.J. Antony, H. Li, et al., Citrus flavonoids as promising phytochemicals targeting diabetes and related complications: a systematic review of in vitro and in vivo studies, *Nutrients* 12 (10) (2020), <https://doi.org/10.3390/nu12102907>.
- [34] D.G. Hong, S. Lee, J. Kim, S. Yang, M. Lee, J. Ahn, et al., Anti-inflammatory and neuroprotective effects of morin in an MPTP-induced Parkinson's disease model, *Int. J. Mol. Sci.* 23 (18) (2022), <https://doi.org/10.3390/ijms231810578>.
- [35] A.D. Kandhare, Z. Liu, A.A. Mukherjee, S.L. Bodhankar, Therapeutic potential of morin in ovalbumin-induced allergic asthma via modulation of SUMF2/IL-13 and BLT2/NF-kB signaling pathway, *Curr. Mol. Pharmacol.* 12 (2) (2019) 122–138, <https://doi.org/10.2174/1874467212666190102105052>.
- [36] Z. Khan, N. Nath, A. Rauf, T.B. Emran, S. Mitra, F. Islam, et al., Multifunctional roles and pharmacological potential of beta-sitosterol: emerging evidence toward clinical applications, *Chem. Biol. Interact.* 365 (2022) 110117, <https://doi.org/10.1016/j.cbi.2022.110117>.
- [37] J. Holbrook, S. Lara-Reyna, H. Jarosz-Griffiths, M. McDermott, Tumour necrosis factor signalling in health and disease, *F1000Res* 8 (2019), <https://doi.org/10.12688/f1000research.17023.1>.
- [38] S. Tukaj, G. Wegrzyn, Anti-Hsp 90 therapy in autoimmune and inflammatory diseases: a review of preclinical studies, *Cell Stress Chaperones* 21 (2) (2016) 213–218, <https://doi.org/10.1007/s12192-016-0670-z>.
- [39] R.F. Zheng, K. Kader, D.W. Liu, W.L. Su, L. Xu, Y.Y. Jin, et al., A network pharmacology approach to decipher the mechanism of total flavonoids from *Dracocephalum Moldavica* L. in the treatment of cardiovascular diseases, *BMC Complement Med Ther* 24 (1) (2024) 15, <https://doi.org/10.1186/s12906-023-04316-x>.
- [40] M.A. Alamri, M. Tahir Ul Qamar, Network pharmacology based virtual screening of Flavonoids from *Dodonaea angustifolia* and the molecular mechanism against inflammation, *Saudi Pharm J* 31 (11) (2023) 101802, <https://doi.org/10.1016/j.jsps.2023.101802>.
- [41] A.G. Dogru, M. Rehders, K. Brix, Investigations on primary cilia of nthy-ori 3-1 cells upon cysteine cathepsin inhibition or thyrotropin stimulation, *Int. J. Mol. Sci.* 24 (11) (2023), <https://doi.org/10.3390/ijms24119292>.
- [42] M. Ferreira, D. Costa, A. Sousa, Flavonoids-based delivery systems towards cancer therapies, *Bioengineering (Basel)* 9 (5) (2022), <https://doi.org/10.3390/bioengineering9050197>.